Proceedings Paper:
Chen, K., Zhang, L. orcid.org/0000-0002-4535-3200 and Zhong, J. (2024) Vertical Handover Strategy in Satellite-Aerial Based Emergency Communication Networks. In: 2024 11th International Conference on Wireless Networks and Mobile Communications (WINCOM). 11th International Conference on Wireless Networks and Mobile Communications, 23-25 Jul 2024, Leeds. IEEE ISBN 979-8-3503-7787-3

https://doi.org/10.1109/WINCOM62286.2024.10657700

Vertical Handover Strategy in Satellite-Aerial Based Emergency Communication Networks

Ke Chen, Li Zhang, Jihai Zhong
School of Electrical and Electronic Engineering
University of Leeds
Leeds, United Kingdom
Email: ml20k2c@leeds.ac.uk, l.x.zhang@leeds.ac.uk, ml18j34z@leeds.ac.uk

***Abstract*—After a disaster, a network of unmanned aerial vehicles (UAVs) and low Earth orbit (LEO) satellites can provide communication services rapidly to the affected area. In this emergency communication system, UAVs frequently encounter network handover (HO) issues while conducting post-disaster situational awareness (SA) tasks such as searching and monitoring during their flight. Due to the high demand for uplink data rates and the time-sensitive nature of sensing data, transmission disconnections are prone to occur if UAVs connect to an inappropriate network, potentially affecting subsequent rescue operations. To tackle this problem, a vertical HO scheme based on the Analytic Hierarch Process-Entropy (AHP-Entropy) weighting and Technique for Order Preference by Similarity to Idea Solution (TOPSIS) is proposed. In this work, received signal strength, data rate, and latency are taken into account. The comprehensive attribute weights are obtained by the AHP-Entropy weighting method, and then TOPSIS is applied to rank the candidates to select the best network. Moreover, the satellite-ground distance is obtained by the Mean Value Theorem for Integrals and the maximum and minimum elevation angles during the movement of LEO satellite. Meanwhile, mobile edge computing (MEC) is introduced on LEO satellite for data compression to further reduce the feeder link delay of LEO satellite. The simulation results show that, compared with the benchmark method, the proposed scheme can significantly improve throughput and reduce disconnections without increasing delay excessively. This ensures the stability and reliability of real-time post-disaster SA.**

***Index Terms*—situational awareness, unmanned aerial vehicles, low Earth orbit satellites, TOPSIS, handover**

I. Introduction

During disasters, the ground network infrastructures, including most base stations (BSs) and power equipment, are often damaged. As a result, they cannot provide communication services, and it is difficult to recover within a short time [1]. Unmanned aerial vehicles (UAVs) can be employed as flying BSs to provide communication services for disaster area [2]. However, due to the limitation of UAVs' battery capacity, this solution cannot provide long-duration services to users. This issue can be overcome by tethered UAVs (TUAVs), which facilitate fiber optical backhaul communication and long endurance by connecting to emergency response vehicles below via fiber optic cables [1].

In practice, effective post-disaster situational awareness (SA) is crucial for post-disaster rescue operations [3]. Since UAVs are flexible and not limited by the destruction of ground roads, post-disaster SA can be performed by UAVs with cameras, which can be used as mobile sensing platforms (MSPs) [4]. SA is typically achieved by data collection and wireless backhaul [3]. A post-disaster emergency communications network consisting of LEO satellites and TUAV-BSs can support multi-user access [1]. However, the inherent high latency of LEO satellites and the constrained bandwidth of TUAV-BSs pose challenges to handover (HO). Due to the high data rate and low latency requirements of sensing data, MSPs are likely to handover to an inappropriate network during movement. This causes excessive latency and disconnection during the data backhaul process. In particular, it is crucial to ensure that sensing data is transmitted from MSPs to the emergency management center with low latency and high reliability. This can greatly improve the efficiency of rescue operations and reduce the damage of disasters to people's lives and property. Therefore, it is of great significance to devise an effective HO scheme to ensure reliable and stable real-time SA in disaster areas.

In the event of a sudden disaster where most BSs are damaged, promptly establishing an emergency communication network can significantly reduce the loss of lives and property. The deployment delay of UAVs was minimized in [2], which ensures timely emergency communication services to be provided to the affected citizens. The work in [5] aimed to address the challenge of processing a large amount of situational information collected by ground terminals (GTs), and investigated multiple collaborative UAVs computation offloading issues with the goal of minimizing computational delay. However, due to the constrained power and bandwidth of UAVs, it is not sufficient to consider a single network of UAVs. The LEO-UAV architecture was proposed in [6], which investigated a scenario in which the UAV-BS provides communication services for people, where the UAV-MEC provides computing services for GTs, and the wide coverage characteristics of LEO satellite can provide cloud computing. The authors maximized the energy efficiency of the system by jointly optimizing resource allocation and UAVs trajectories. Considering the challenge of the short battery life of UAVs, the authors in [7] proposed a satellite-aerial architecture including high-altitude platforms (HAPs) and one LEO satel-

979-8-3503-7786-6/24/$31.00 © 2024 IEEE

lite. Nevertheless, it is prone to cause network load imbalance in the space-air network, which leads to decreased quality of services (QoS). In [8], the authors investigated the user network selection problem in LEO-UAVs network, which is modeled as an evolutionary game problem that well-balanced the space-air network, thereby ensuring the QoS in the post-disaster area.

Although there have been many studies about the emergency communication system built by satellites, UAVs, and HAPs in post-disaster scenarios, most researchers focused on providing communication and computation services to ground users and terminals, often neglecting aerial users. Furthermore, the HO problem faced in the process of post-disaster SA is almost ignored. To the best of our knowledge, the HO problem in heterogeneous network when MSPs conduct post-disaster SA has not been studied. In this paper, we propose a TOPSIS-based [9] vertical HO scheme for SA in post-disaster scenarios. The main contributions of this paper are summarized as follows.

- For disaster SA conducted by MSPs, we consider the high data rate demand of uplink and the time-sensitive nature of the sensing task. An AHP-Entropy and TOPSIS (AE-TOPSIS) scheme is proposed to make vertical HO decisions to ensure reliable and stable real-time disaster SA.
- For high-speed moving LEO satellites, the Iridium-based parameters are used in this work [10]. Meanwhile, a satellite-ground distance calculation method is proposed based on the Mean Value Theorem for Integrals [11], which characterizes the effect of the satellite movement on the system.
- The proposed method is evaluated by simulation. Numerical results show that, compared with the RSS-based method [12] and the Entropy weighting-TOPSIS method, the method proposed in this paper can obtain a higher throughput without increasing delay, and can greatly reduce the disconnection rate of the transmission.

II. System Model

After a disaster occurs, we consider an emergency scenario in which most terrestrial BSs and power equipment are destroyed, as shown in Fig. 1. We assume there are K TUAV-BSs hovering in the air with a fixed height H. They provide wireless coverage for K victim clusters in the area. The number of people in each cluster varies and is denoted as n_i for the ith cluster, $i \in \{1, 2, ..., k\}$. The numbers of all k clusters are collected in a set $\mathcal{N} = \{n_1, ..., n_k\}$. Victim clusters and TUAV-BSs are distributed following Poisson cluster distribution. Considering a LEO satellite covers the area for a finite time horizon T, while one MSP moves along a randomly generated trajectory within the area during T to conduct the SA task. Vertical HO occurs when the MSP passes through the overlapping coverage of TUAV-BSs and the LEO satellite. To ensure a reliable and low-latency sensing data transmission, the MSP needs to connect to a suitable network.

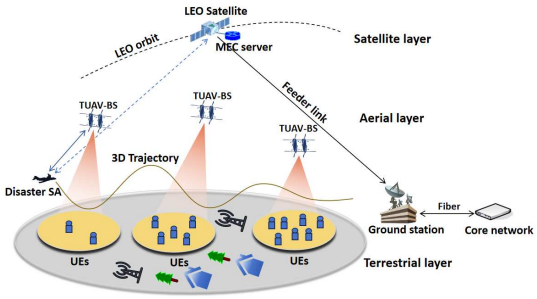

Fig. 1. Schematic diagram of SA in the disaster scenario

A. UAV Trajectory

Assuming the period T is discretized into M equal time slots, indexed by $m = 1, ..., M$. Without loss of generality, we consider the use of a 3D Cartesian coordinate system in this model. The location of the MSP can be represented as $p[m] = (x[m], y[m], z[m])$, while TUAV-BSs' coordinate can be denoted as $p_k = (x_k, y_k, z_k)$. Assuming that the speed of MSP in the x, y, and z directions can be independently controlled. And the maximum speeds are V^x_{max}, V^y_{max}, and V^z_{max} respectively. V_x, V_y and V_z are randomly generated from 0 to their maximum value. The start point of MSP is randomly generated in the area, after M time slots, a trajectory is generated.

B. Channel Model

In this paper, we consider the MSP connect to TUAV-BS or the LEO satellite via Air-to-Air (A2A) channel and Air-to-Space (A2S) channel respectively. According to the non-terrestrial networks (NTN) channel models in 3GPP TR 38.811 [13], different carrier frequencies have different ionospheric attenuation, tropospheric attenuation, and atmospheric gas attenuation, all of which impact the NTN path loss.

1) A2A Channel Model: Most of the buildings in the area are destroyed due to the disaster, so the A2A channel will be line-of-sight (LOS) communication link. We adopt a channel fading model with free-space path loss. With this channel model, the path loss between MSP and kth TUAV-BS at slot m is

$$PL_{m,k} = \left(\frac{4\pi f_k d_{m,k}}{c}\right)^{\xi^1} \tag{1}$$

where c is the speed of light, f_k is the carrier frequency of TUAV-BS k, $\xi^1 = 2$ is the path loss exponent, $d_{m,k} = \sqrt{(x[m]-x_k)^2 + (y[m]-y_k)^2 + (z[m]-z_k)^2}$ is the distance between MSP to kth TUAV-BS at slot m.

2) A2S Channel Model: Since LEO satellites are always moving at high speeds, each LEO satellite can only maintain communications for about few minutes with the users in its coverage [13]. The distance for A2S link varies based on different elevation angles. We consider the Iridium communication satellite in this paper, which has an inclination of

86.4° [10], and it can cover almost the entire Earth's surface. As shown in Fig. 2, we assume that when $t = 0$, the elevation angle from the ground station to the LEO satellite is $\theta = \theta_{min}$. At this time, the satellite has the maximum distance to the ground station $D = D_{max}$. During the movement of the satellite along its orbit, when $t = \frac{1}{2}T$, and the subsatellite point of the satellite coincides with the ground station. Hence the elevation angle is $\theta = \theta_{max} = \frac{1}{2}\pi$. The distance between the satellite and ground is minimal $D = D_{min} = h_0$, where h_0 is the height of the LEO satellite. Applying cosines law and simplifying, the distance between the satellite and the ground station can be expressed as [13]

$$D = \sqrt{(R_E \sin\theta)^2 + h_0^2 + 2h_0 R_E} - R_E sin\theta \qquad (2)$$

where R_E is Earth radius, θ is the elevation angle. Applying

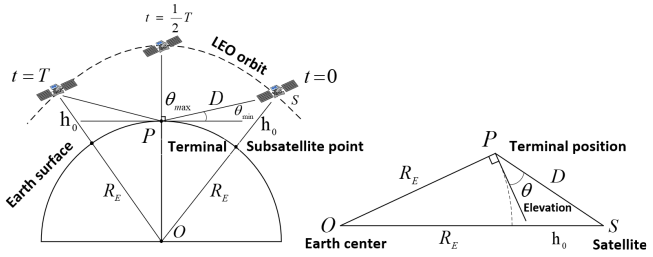

Fig. 2. Space-ground distance during LEO satellite movement

the Mean Value Theorem for Integrals to obtain the average distance from space to ground during the movement of the satellite, which can be represented by

$$\overline{D} = \frac{1}{\theta_{max} - \theta_{min}} \int_{\theta_{min}}^{\theta_{max}} (\sqrt{(R_E \sin\theta)^2 + h_0^2 + 2h_0 R_E} - R_E sin\theta) \mathrm{d}\theta \qquad (3)$$

Iridium satellite parameters are used in this paper, and the carrier frequency of the satellite is L-band [10], which has a high capacity to penetrate the atmosphere and rainwater. Therefore for A2S channel, we adopt a channel fading model by integrating free space path loss and Ionospheric scintillation loss. Meanwhile, we assume the ground station is close to the affected area. Hence $\overline{d_s} \approx \overline{D}$, where $\overline{d_s}$ is the average distance from the satellite to the area during period T. The path loss for A2S link is

$$PL_s = \left(\frac{4\pi f_s \overline{d_s}}{c}\right)^{\xi^2} + l_i \qquad (4)$$

where f_s is the carrier frequency of the LEO satellite, ζ^2 is the path loss exponent, l_i is the Ionospheric scintillation loss caused by the effect of Ionospheric scintillation on the wireless signal.

C. Transmission Model

In the coverage of a LEO satellite and TUAV-BSs, and vertical HO may occur during the mobility of the MSP. The traditional method cannot meet the vertical HO as it only considers one attribute. Hence, it is important to adopt a HO scheme that considers multiple criterion to ensure reliable and stable real-time post-disaster SA. This section analyzes the metrics of each network that affect the data transmission performance of the MSP, including received signal strength (RSS), data rate, and latency.

1) Received Signal Strength: For A2A link, the RSS from MSP to kth TUAV-BS at slot m is

$$RSS_{m,k} = P^t_{u\to u} + G^t_u + G^r_u - PL_{m,k} \qquad (5)$$

where $P^t_{u\to u}$ is the transmit power from MSP to TUAV-BS, $PL_{m,k}$ is the path loss of this link, G^t_u and G^r_u are the antenna gains of transmitter and receiver. Since the limited payload capacity of UAVs, G^t_u and G^r_u are set to 0 here. For A2S link, the RSS between MSP and satellite is

$$RSS_s = P^t_{u\to s} + G^t_u + G^r_s - PL_s \qquad (6)$$

where PL_s is the path loss of the A2S link, $P^t_{u\to s}$ is the transmit power from MSP to the LEO satellite, G^r_s is the receiver antenna gain of the satellite. Note that, the satellite can carry antennas with sufficiently large antenna gain to overcome large path loss due to long propagation distance.

2) Data Rate: We assume that the bandwidth resource of different networks is divided equally among the users served. Different TUAV-BSs adopt different frequencies in this paper. In other words, the interference between different TUAV-BSs can be avoided. For A2A link, the signal carrier-to-noise ratio between MSP and kth TUAV-BS at slot m is

$$SNR_{m,k} = \frac{P^t_{u\to u} G^t_u G^r_u}{K_B T_s B_k PL_{m,k}} \qquad (7)$$

where B_k is the bandwidth allocated to the MSP after connecting to TUAV-BS k, and its value is $B_k = \frac{B_U}{n_k}$, where B_U is the total bandwidth of each TUAV-BS. K_B is Boltzmann constant and T_s is the system noise temperature. For A2S link, the signal carrier-to-noise ratio is

$$SNR_s = \frac{P^t_{u\to s} G^r_s G^r_u}{K_B T_s B_S PL_s} \qquad (8)$$

where B_S is the bandwidth of the LEO satellite. According to the Shannon formula, the data rate for the A2A link and A2S link are calculated as

$$R_{m,k} = B_k log_2(1 + SNR_{m,k}) \qquad (9)$$

$$R_s = B_S log_2(1 + SNR_s) \qquad (10)$$

3) Delay: For the LEO satellite network, the total delay consists of fronthaul uplink and feeder link delay, and each link delay includes transmission delay and propagation delay. To reduce feeder link delay, we assume that the mobile edge computing is carried on the LEO satellite in this paper. Once the satellite receives a large amount of data transmitted from the MSP, it is compressed and processed, and then forwarded to the ground station by feeder link. In this way, the transmission delay of the feeder link can be ignored. Hence the total delay of the LEO satellite is

$$t_s = \frac{P_A}{R_s} + \frac{2\overline{d_s}}{c} \qquad (11)$$

where P_A is the size of transmission data packet.

For A2A link, we only need to consider transmission delay, thereby the total delay of A2A link can be expressed as $t_{m,k} = \frac{P_A}{R_{m,k}}$.

III. Handover Strategy Based on Subjective-objective Weighting and TOPSIS

In the process of SA in this paper, the MSP moving through the coverage areas of the LEO satellite and some TUAV-BSs, will choose a suitable network to connect. The traditional RSS-based scheme, which only considers a single criterion, often results in the MSP connecting to a nearby TUAV-BS that cannot provide the required data rate. Therefore, there is a great possibility of transmission failure, which consequently affects the rescue tasks. The multi-attribute decision making (MADM) [12] method can utilize multiple criterion of the heterogeneous network to make decisions, which can realize effective HO to ensure highly reliable, stable and low-latency SA in the post-disaster areas.

A. Establishment of MADM Matrix

The first step of the MADM-based vertical HO is to establish an MADM decision matrix based on candidate BSs. The MSP measures RSS from the neighboring TUAV-BSs. If the RSS exceeds a threshold, then these TUAV-BSs are considered as candidate BSs. In this paper, RSS, data rate and delay are used as criterion for vertical HO. Hence, the decision matrix A can be represented by

$$A = \begin{bmatrix} a_{11} & a_{12} & a_{1q} \\ a_{21} & a_{22} & a_{2q} \\ \vdots & \vdots & \vdots \\ a_{p1} & a_{p2} & a_{pq} \end{bmatrix} \tag{12}$$

where p is the number of candidate BSs, $p = 0, 1, \cdots, K$, and q is the number of attributes, $q = 1, \cdots, 3$, representing RSS, data rate, and delay attributes respectively. a_{ij} represents the jth attribute value corresponding to the ith candidate.

Since different attributes have different scales, they are all normalized. Data rate and RSS are benefit types of attributes, which are the higher the better, so they are normalized by (13). Delay is the cost type of attribute, which is the lower the better, so it is normalized by (14).

$$d_{ij} = \frac{a_{ij} - \min\limits_{j}(a_{ij})}{\max\limits_{j}(a_{ij}) - \min\limits_{j}(a_{ij})} \tag{13}$$

$$d_{ij} = \frac{\max\limits_{j}(a_{ij}) - a_{ij}}{\max\limits_{j}(a_{ij}) - \min\limits_{j}(a_{ij})} \tag{14}$$

B. Calculate the Attribute Weight

In MADM, attribute weights are used to quantitatively represent the importance of attributes, which can be determined by either subjective weighting or objective weighting. However, both methods are one-sided. In order to make better trade-offs between the RSS, data rate and delay, this paper integrates the subjective and objective weighting methods to obtain more comprehensive attribute weights.

1) Compute Weight Based on Entropy Method: The entropy method can be used to calculate objective weights for attributes. The weight of each attribute is obtained directly from the decision matrix.

Step 1: The decision matrix after normalization is used to calculate the proportion of the jth attribute in the ith candidate BS out of the total candidate BSs, which can be calculated by $p_{ij} = \frac{d_{ij}}{\sum_{j=1}^{p} d_{ij}} (j = 1, 2, .., q)$.

Then the entropy of the jth attribute can be obtained by $e_j = -k * \sum_{i=1}^{p} p_{ij} ln(p_{ij})$, where k is the coefficient, and the value is $\frac{1}{ln(p)}$. The deviation of the jth attribute is $g_j = 1 - e_j$. Higher value indicates the attribute is more significant.

Step 2: The objective weight of the jth attribute can be obtained by $w_j^o = \frac{g_j}{\sum_{j=1}^{q} g_j}$.

2) Calculate Weight Based on AHP Method: AHP is an effective subjective weighting method that has been widely used in MADM problems [12]. The AHP-based weighting calculation process is explained in the following.

Step 1: A pair-wise comparison matrix can be constructed according to Satty's 9-1 scale rule [14]. The more important the attribute, the larger the number it corresponds to. These numbers range from 1-9. Therefore, the pair-wise comparison matrix can be described as

$$P = \begin{bmatrix} x_{11} & x_{12} & \cdots & x_{1q} \\ x_{21} & x_{22} & \cdots & x_{2q} \\ \vdots & \vdots & \ddots & \vdots \\ x_{q1} & x_{q2} & \cdots & x_{qq} \end{bmatrix} \tag{15}$$

where x_{ij} is the relative importance of the ith attribute compared to the jth attribute, which can be obtained from Saaty's importance scale rule [14]. When $i = j$, $x_{ij} = 1$, and when $i \neq j$, $x_{ji} = \frac{1}{x_{ij}}$.

Step 2: The maximum eigenvalue λ_{max} can be obtained by $det(P - I\lambda) = 0$, where I is the unit matrix.

Step 3: The consistency of the pairwise comparison is checked to ensure the constructed pair-wise comparison matrix is reasonable and consistent. The consistency index (CI) can be obtained by $CI = \frac{\lambda_{max} - q}{q-1}$, where q is the number of attributes. Therefore the consistency ratio (CR) can be calculated by $CR = \frac{CI}{RI}$, where RI is the random consistency index [14]. If $CR < 0.1$, it illustrates that the pair-wise comparison matrix is accepted.

Step 4: The subjective weights can be calculated by

$$\begin{aligned} PW^s &= \lambda_{max} W^s \\ W^s &= (w_1^s, .., w_q^s)^T \end{aligned} \tag{16}$$

where W^s is the subjective weight vector.

3) Compute the Combination Weight: To better trade off the multiple attributes of the candidate network, this paper integrates the subjective and objective weights of attributes to obtain the comprehensive weight, which is $w_j = \alpha w_j^s + \beta w_j^o$, where α and β are the weight coefficients, and we take $\alpha = \beta = 0.5$ in this paper.

C. Rank Candidate BSs Based on TOPSIS

After obtaining the comprehensive weight of attributes, rank the candidate BSs according to TOPSIS and select the

Algorithm 1 Handover Scheme Based on AE-TOPSIS

initialize the decision matrix A and weights w_j
for each $m \in [1, M]$ **do**
  if $RSS_m < RSS_{threshold}$ **then**
    the MSP connect to the LEO satellite
  else
    construct decision matrix A based on candidate BSs, and normalized it by (13) and (14)
    get objective weights $w_j^o = \frac{g_j}{\sum_{j=1}^{q} g_j}$
    get subjective weights by (16), and obtain comprehensive weights by $w_j = \alpha w_j^s + \beta w_j^o$
    $r_i = \frac{d_i^-}{d_i^+ + d_i^-}$, after calculating the relative proximity of all candidate BSs, get vector R
    $HO_t = \underset{i \in p}{argmax} R(i)$, choose the maximum value corresponding to the candidates as target BS
  end if
end for

highest ranked BS as the new HO target, which includes the following steps.

Step 1: Calculate the weighted normalized decision matrix. Each element of the normalized decision matrix is weighted, so we get $v_{ij} = w_j d_{ij}$, $i = 1, 2, ...p$, $j = 1, 2, ...q$, as the element of the weighted normalized decision matrix V.

Step 2: Obtain the positive ideal solution V^+ and the negative ideal solution V^- based on the weighted normalized decision matrix V, the ideal solutions are given as

$$V^+ = \left\{ (\underset{i \in p}{max} V_{ij} \mid j \in J^+), (\underset{i \in p}{min} V_{ij} \mid j \in J^-) \right\} = \{v_1^+, ..., v_q^+\} \tag{17}$$

$$V^- = \left\{ (\underset{i \in p}{max} V_{ij} \mid j \in J^-), (\underset{i \in p}{min} V_{ij} \mid j \in J^+) \right\} = \{v_1^-, ..., v_q^-\} \tag{18}$$

where J^+ is the attributes set with positive impact, J^- is the attributes set with negative impact.

Step 3: Obtain the Euclidean distance by (19) and (20)

$$d_i^+ = \sqrt{\sum_{j=1}^{q} (d_{ij} - v_j^+)^2} \tag{19}$$

$$d_i^- = \sqrt{\sum_{j=1}^{q} (d_{ij} - v_j^-)^2} \tag{20}$$

where d_i^+ is the Euclidean distance of each candidate from positive ideal solution V^+, and d_i^- is the Euclidean distance of each candidate from negative ideal solution V^-.

Step 4: Compute the relative proximity to the ideal solutions, which can be calculated by $r_i = \frac{d_i^-}{d_i^+ + d_i^-}$.

Step 5: All the candidates are ranked based on their relative proximity to the ideal solution in increasing order. The top one is selected as the target, that is, $HO_t = \underset{i \in p}{argmax} R(i)$, where R is the ranking vector.

IV. Simulation and Performance Analysis

In this section, we present simulation results in terms of system sum rate, delay, HO, and disconnection ratio to evaluate the performance of the HO scheme of the MSP in a post-disaster area. We assume a 1000m×1000m scenario. To avoid interferences between different TUAV-BSs, each TUAV-BS is assigned to an orthogonal sub-channel with an equal bandwidth of 1MHz at 2GHz bands. The Iridium-based constellation parameters are used in this paper. The details of rest parameters based on [10] [13] are given in the Table I.

TABLE I
Simulation Parameters

Parameter	Value	Parameter	Value
T	10min	M	200
c	3×10^8 m/s	V_{max}^x	10m/s
V_{max}^y	10m/s	V_{max}^z	5m/s
θ_{min}	8.2°	h_0	780km
R_E	6371km	f_s	1.6GHZ
B_s	10MHZ	$P_{u \to u}^t$	23dBm
$P_{u \to s}^t$	33dBm	T_s	300K
G_s^r	30dBi	l_i	7dB

Fig. 3 evaluates the overall sum rate and average delay for different HO schemes. The average system delay is obtained by dividing the total delay by the total time slot M. The figure on the left shows the average delay results of four schemes, i.e. satellite, AE-TOPSIS, Entropy-TOPSIS (E-TOPSIS) [15], and baseline. In the satellite scheme, the MSP always connects to the LEO satellite. And the baseline scheme is the RSS-based HO. It can be observed that the satellite-based scheme incurs the largest delay among the four schemes, significantly more than the other three schemes. The scheme proposed in this paper has only a slight increase compared to the baseline scheme, which has the lowest delay. The right figure shows the system sum rate results utilizing the four schemes, and shows that the scheme proposed in this paper is significantly higher than the baseline scheme and also slightly higher than the E-TOPSIS scheme, while slightly lower than the satellite scheme which has the highest sum rate. Therefore, a good trade-off between delay and sum rate has been achieved.

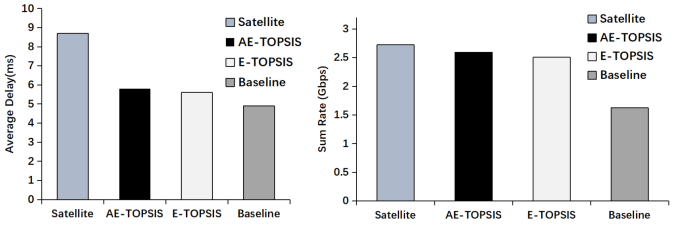

Fig. 3. System sum rate and average delay of different schemes

Fig. 4 depicts the system HO and disconnection ratio of the three schemes. HO ratio is defined as $R_{HO} = \frac{N_{HO}}{M}$, where N_{HO} is the number of HO for the MSP during the flight, and the disconnection ratio can be calculated by

$R_{dis} = t_{dis}/T$, where t_{dis} is the time of disconnection. When the MSP handover to a TUAV-BS, if the newly connected TUAV-BS cannot achieve the required data rate, that is $R_{new} < R_{threshold}$, then it will cause the disconnection. Since the MSP needs to transmit a large amount of rate-demanding sensing data, including high-definition video, etc., here we set the $R_{threshold}$ to 6Mbps. It can be seen that the scheme proposed in this paper reduces the HO number and disconnection ratio compared to the baseline scheme. Besides, the scheme also outperforms E-TOPSIS. With the baseline scheme, the MSP may switch to a nearby TUAV-BS during flight. If the TUAV-BS has served a larger number of users, and thus it is impossible to provide sufficient bandwidth to the MSP. Note, in general, TUAV-BSs typically offer higher data rates for downlink than for uplink, which makes it difficult to meet the high demand for uplink data rates required by the MSP.

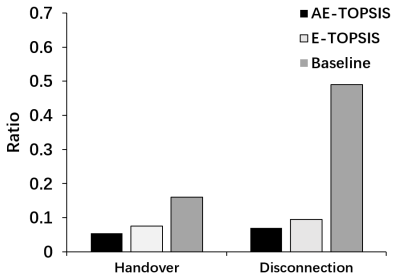

Fig. 4. System HO and disconnection ratio of different schemes

Fig. 5 compares the overall sum rate and disconnection ratio of the three schemes considering different packet sizes. It can be clearly seen that the proposed scheme is markedly better than the baseline scheme for all packet sizes, and slightly better than the E-TOPSIS scheme. LEO satellites have a larger bandwidth and large antenna gain compared to TUAV-BSs, resulting in better transmission rates for A2S links than that of the TUAV-BSs. However, the propagation delay of the A2S link is too high, which results in much higher transmission delay compared to the A2A links. As the packet size increases, the transmission delay of different links is affected, and we can observe that the total delay of the A2S link gradually approaches to or is even lower than that of the A2A link, which affects the HO strategy and ultimately the performance of the system. The performance of the baseline method shows fluctuations with insignificant change, as the baseline method neglects the data rate and delay of system performance metrics.

V. Conclusion

In this paper, we propose a TOPSIS-based vertical HO method to ensure reliable and stable real-time post-disaster SA. Specifically, we model the MSP HO as a MADM problem, considering the RSS, delay, and data rate requirements of the post-disaster SA. The comprehensive weights of the system attributes are obtained by subjective and objective

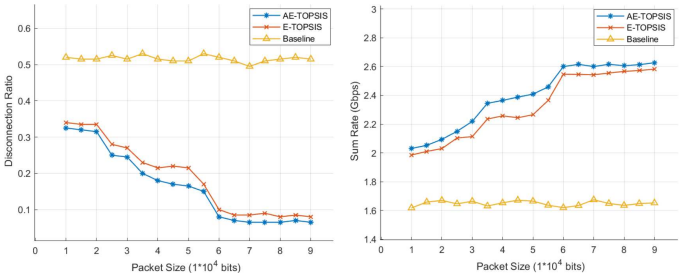

Fig. 5. System performance of different packet sizes

weighting methods. Subsequently, the TOPSIS algorithm is applied to rank candidate BSs. The simulation results demonstrate that the proposed scheme can significantly reduce the disconnection ratio and increase the throughput of the MSP without compromising much the delay during post-disaster SA operations. This further improves the efficiency of post-disaster rescue operations.

References

[1] L. Zhen, "Research on Space-Air-Ground Integrated Emergency Communication Networks," *Mobile Communications*, 2022,46(10): 47-52.

[2] X. Zhang and L. Duan, "Optimization of Emergency UAV Deployment for Providing Wireless Coverage," *GLOBECOM 2017 - 2017 IEEE Global Communications Conference*, Singapore, 2017, pp. 1-6.

[3] R. Geraldes et al., "UAV-Based Situational Awareness System Using Deep Learning," *IEEE Access*, vol. 7, pp. 122583-122594, 2019.

[4] H. Hildmann, E. Kovacs, "Review: Using Unmanned Aerial Vehicles (UAVs) as Mobile Sensing Platforms (MSPs) for Disaster Response, Civil Security and Public Safety," *Drones*, 2019, 3, 59.

[5] C. Chen, T. Zhang, W. Xu, X. Yang and Y. Wang, "Multi-UAV Cooperation Based Edge Computing Offloading in Emergency Communication Networks," *2023 IEEE Wireless Communications and Networking Conference (WCNC)*, United Kingdom, 2023, pp. 1-6.

[6] Z. Hu et al., "Joint Resources Allocation and 3D Trajectory Optimization for UAV-Enabled Space-Air-Ground Integrated Networks," in *EE Transactions on Vehicular Technology*, vol. 72, no. 11, pp. 14214-14229, Nov. 2023.

[7] L. Zhang, H. Zhang, C. Guo, H. Xu, L. Song and Z. Han, "Satellite-Aerial Integrated Computing in Disasters: User Association and Offloading Decision," *ICC 2020 - 2020 IEEE International Conference on Communications (ICC)*, Dublin, Ireland, 2020, pp. 554-559.

[8] S. Yan, L. Qi and M. Peng, "User Access Mode Selection in Satellite-Aerial Based Emergency Communication Networks," *2018 IEEE International Conference on Communications Workshops (ICC Workshops)*, Kansas City, MO, USA, 2018, pp. 1-6.

[9] Alhabo. M, Zhang. L, Nawaz. N, "Energy Efficient Handover for Heterogeneous Networks: A Non-Cooperative Game Theoretic Approach," *Wireless Personal Communications*, 122 (3). pp. 2113-2129.

[10] Y. C. Hubbel, "A comparison of the IRIDIUM and AMPS systems," *IEEE Network*, vol. 11, no. 2, pp. 52-59, March-April 1997.

[11] E. T. Whittaker, G. N. Watson, A Course of Modern Analysis Fifth Edition, Cambridge University Press, 2021.

[12] M. Kassar, B. Kervella, and G. Pujolle, "An overview of vertical handover decision strategies in heterogeneous wireless networks," *Computer Communications*, vol. 31, no. 10, pp. 2607–2620, Jun. 2008.

[13] 3GPP, "Study on new radio (nr) to support non-terrestrial networks (release 15): Ts 38.811," 2018.

[14] Y. Zhong, H. Wang, H. Lv, and F. Guo, "A vertical handoff decision scheme using subjective-objective weighting and grey relational analysis in cognitive heterogeneous networks," *Ad Hoc Networks*, vol. 134, p. 102924, Sep. 2022.

[15] K. Xiao, C. Li, "Vertical Handoff Decision Algorithm for Heterogeneous Wireless Networks Based on Entropy and Improved TOPSIS," *2018 IEEE 18th International Conference on Communication Technology (ICCT)*, Chongqing, China, 2018, pp. 706-710.